Inorg. Chem. **2003**, *42*, 6114–6122

Structural, Electrical, and Magnetic Properties of a Series of Molecular Conductors Based on BDT-TTP and Lanthanoid Nitrate Complex Anions (BDT-TTP = 2,5-Bis(1,3-dithiol-2-ylidene)-1,3,4,6-tetrathiapentalene)

Hengbo Cui,[†,‡] Takeo Otsuka,[†] Akiko Kobayashi,*[,†] Naoya Takeda,[§] Masayasu Ishikawa,[§] Yohji Misaki,[||] and Hayao Kobayashi[‡]

Research Centre for Spectrochemistry, Graduate School of Science, The University of Tokyo, Hongo, Bunkyo-ku, Tokyo 113-0033, Japan, Institute for Solid State Physics, The University of Tokyo, Kashiwa, Chiba 277-85821, Japan, Department of Molecular Engineering, Graduate School of Engineering, Kyoto University, Yoshida, Kyoto 606-8501, Japan, and Institute for Molecular Science and CREST, Okazaki 444-8585, Japan

Received May 1, 2003

The platelike crystals of a series of novel molecular conductors, which are based on the π-donor molecules BDT-TTP (2,5-bis(1,3-dithiol-2-ylidene)-1,3,4,6-tetrathiapentalene) with a tetrathiapentalene skeleton and lanthanide nitrate complex anions $[Ln(NO_3)_x]^{3-x}$ (Ln = La, Ce, (Pr), Tb, Dy, Ho, Er, Tm, Yb, Lu) with localized 4f magnetic moments, were synthesized. Except for the Ce complex, the salts were composed of $(BDT\text{-}TTP)_5[Ln(NO_3)_5]$ and were isostructural. Even though the Ce crystal had a different composition, $(BDT\text{-}TTP)_6[Ce(NO_3)_6](C_2H_5OH)_x$ ($x \approx 3$), the crystals all had the space group $P\bar{1}$. Although the X-ray examination of the Pr salts was insufficient, the existence of two modifications was suggested in these systems by preliminary X-ray examination. Previously, we reported the crystal structures and unique magnetic properties of $(BDT\text{-}TTP)_5[Ln(NO_3)_5]$ (Ln = Sm, Eu, Nd, Gd). Thus, by combining the results of this work with previous one, we for the first time succeeded in obtaining a complete set of organic conductors composed of the identical π-donors (BDT-TTP in this case) and all the lanthanide nitrate complex anions (except the complex with Pm^{3+}). The crystals were all metallic down to 2 K. Electronic band structure calculations resulted in two-dimensional Fermi surfaces, which was consistent with their stable metallic states. Except for the Lu complex, which lacked paramagnetic moments, the magnetic susceptibilities were measured on the six heavy lanthanide ion complex salts by a SQUID magnetometer (Ln = Tb, Dy, Ho, Er, Tm, Yb). The large paramagnetic susceptibilities, which were caused by the paramagnetic moments of the rare-earth ions, were obtained. The Curie–Weiss law fairly accurately reproduced the temperature dependence of the magnetic susceptibilities of $(BDT\text{-}TTP)_5[Ho(NO_3)_5]$ in the experimental temperature range (2–300 K) and a comparatively large Weiss temperature ($|\Theta|$) was obtained (Θ(Ho) = –15 K). A Weiss temperature (Θ(Tm) = –8 K) was also obtained for Tm. The $|\Theta|$ values of other $(BDT\text{-}TTP)_5[Ln(NO_3)_5]$ salts and $(BDT\text{-}TTP)_6[Ce(NO_3)_6](C_2H_5OH)_x$($x \approx 3$) were as follows: $|\Theta|/K$ = 4 (Er), $\leq$2 (Ce, Tb, Dy, Yb). The comparatively strong intermolecular magnetic interaction between Ho^{3+} ions, which was suggested by the $|\Theta|$ value, is inconsistent with the traditional image of strongly localized 4f orbitals shielded by the electrons in the outer 5s and 5p orbitals. The dipole interactions between Ln^{3+} ions causing the Curie–Weiss behavior and the comparatively large Θ value of $(BDT\text{-}TTP)_5[Ho(NO_3)_5]$ is inconsistent with the data, since the complexes exhibit isostructural properties and there is not a clear relationship between the magnitudes of Θ values and those of magnetic moments. Therefore, it is possible that the 4f orbitals of Ho atom are sensitive to the ligand field, which will have an effect on the orbital moment of the Ho^{3+} ion and/or produce a small amount of mixing between 4f and ligand orbitals to give rise to "real" intermolecular antiferromagnetic interaction through intermolecular overlapping between π (BDT-TTP) and ligand orbitals of lanthanide nitrate complex anions.

Introduction

Since the discovery of the first organic superconductor in 1980,[1] numerous molecular metals and superconductors have been reported.[2,3] Although the highest T_c value of an organic superconductor was recently reported using high pressure and β'-$(BEDT\text{-}TTF)_2ICl_2$ (T_c = 14 K at 8 GPa),[4] the development of plain organic superconductors with simple

* To whom correspondence should be addressed. E-mail: akiko@chem.s.u-tokyo.ac.jp. Tel (fax): +81-3-5841-4417.

† Research Centre for Spectrochemistry, Graduate School of Science, The University of Tokyo.

‡ Institute for Molecular Science and CREST.

§ Institute for Solid State Physics, The University of Tokyo.

|| Kyoto University.

10.1021/ic034459g CCC: $25.00
Published on Web 08/23/2003

π electrons is somewhat stagnant. In contrast, a great deal of research has recently concentrated on developing magnetic molecular conductors. It is believed that molecular conductors, whose conducting properties can be sharply altered by external forces (or stimuli) such as a magnetic field and irradiation with visible light, will be crucial in the conduction function of molecular systems.[5] In 1995, Kurmoo et al. reported a paramagnetic organic superconductor, β''-(BEDT-TTF)$_4$(H$_2$O)Fe(C$_2$O$_4$)$_3$(C$_6$H$_5$CN) (BEDT-TTF = bis(ethylenedithio)tetrathiafulvalene),[6] and Coronado et al. reported the first organic metal with ferromagnetic anion layers, (BEDT-TTF)$_3$[MnCr(C$_2$O$_4$)$_3$]$_2$.[7] However, even in these prominent systems the coupling between magnetic moments and conduction electrons appeared to be weak and distinct dual-functional properties were hardly observed. We previously prepared magnetic organic conductors based on BETS (=bis(ethylenedithio)tetraselenafulvalene) and typical magnetic anions, FeX_4^- (X = Cl, Br), and found many unprecedented electromagnetic properties that originated from the interplay between conductivity and magnetism.[8,9] For example, the coexistence of the three-dimensional (antiferro)magnetic order and organic superconductivity was first realized in κ-(BETS)$_2$FeBr$_4$.[10] The antiferromagnetic superconducting state can be sharply switched on or off by controlling the external magnetic field due to the metamagnetic nature of the complex.[11] In addition, field-induced superconducting transitions were discovered, which were also observed in a similar BETS conductor, λ-(BETS)$_2$FeCl$_4$.[12,13] In the system with diluted Fe^{3+} ions, λ-(BETS)$_2$Fe$_x$Ga$_{1-x}$Cl$_4$ ($0.3 < x < 0.5$) exhibited a superconductor-to-insulator transition in a zero magnetic field.[14] The unprecedented insulator−superconductor−metal switching was realized by slightly tuning the external magnetic field.[11] Though these electromagnetic phenomena were realized only at low temperature, these findings suggest the latent possibility of organic conductors with magnetic anions. Since these other works used systems with the 3d magnetic moments, we have tried to prepare organic metals with 4f magnetic moments. Although there is not an example of an isostructural series of organic metals with identical π donors and various 3d transition-metal ions (M^{n+}; M = Sc, Ti, V, Cr, Mn, Fe, Co, Ni, Cu), developing a series of organic metals with lanthanide ions, Ln^{3+} (Ln = Ce, Pr, Nd, (Pm), Sm, Eu, Gd, Tb, Dy, Ho, Er, Tm, Yb, Lu), will be much easier because of the similar nature of lanthanide ions. Furthermore, in comparison to 3d elements, the 4f elements, namely lanthanides, are expected to show distinctive magnetic properties due to the coexistence of electron spins and the large 4f orbital moments. To date there have been insufficient syntheses and characterization of molecular metals containing lanthanide complex anions. Several years ago Imakubo et al. reported the first metallic conductors with rare-earth chloride complexes, but the conductors were not very air stable and the crystal structures were not determined.[15] On the other hand, stable heavy rare-earth complex anions, $[Ln(NCS)_6]^{3-}$ (Ln = Ho, Er, Yb, Y), yielded stable (BEDT-TTF)$_4$[Ln(NCS)$_6$]-CH$_2$Cl$_2$ salts.[16] Although their structural and magnetic properties were studied, they are insulating. Recently, several metallic compounds were synthesized using the organic donors BEDO-TTF (or BO) (bis(ethylenedioxy)tetrathiafulvalene), BDT-TTP (2,5-bis(1,3-dithiol-2-ylidene)-1,3,4,6-tetrathiapentalene), and DIEDO (diiodo(ethylenedioxy)-tetrathiafulvalene) with $[Ln(NCS)_6]^{3-}$ (Ln = Ho, Er, Yb, Y); the $[Ln(NCS)_6]^{3-}$ layers were disordered, except in the (DIEDO)$_6$[Ln(NCS)$_6$] salt.[17] The full characterization of these metal systems is fairly difficult, since the anionic layers are frequently disordered. On the other hand, Kushch et al. reported the synthesis, crystal structure, and semiconducting properties of (BEDT-TTF)$_5$[Dy(NCS)$_6$NO$_3$]C$_2$H$_5$OH.[18] More recently, we synthesized new organic conductors (BDT-TTP)$_5$[Ln(NO$_3$)$_5$] (Ln = Nd, Sm, Eu, Gd) and briefly

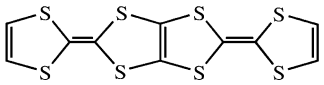

BDT-TTP[2,5-bis(1,3-dithiol-2-ylidene)-1,3,4,6-tetrathiapentalene]

(1) Jérome, D.; Mazaud, M.; Ribault, M.; Bechgaard, K. *J. Phys. Lett.* **1980**, *41*, L95−L98.
(2) Williams, J. M.; Ferraro, J. R.; Thorn, R. J.; Carlson, K. D.; Geiser, U.; Wang, H. H.; Kini, A. M.; Whangbo, M.-H. *Organic Superconductors*; Prentice Hall: Englewood Cliffs, NJ, 1992.
(3) Cassoux, P.; Valade, L.; Kobayashi, H.; Kobayashi, A.; Clark, R. A.; Underhill, A. E. *Coord. Chem. Rev.* **1991**, *110*, 115−160.
(4) Taniguchi, H.; et al. Private communications (see also: Adachi, T.; Ojima, E.; Zhang, B.; Narymbetov, Kobayashi, H.; Miyazaki, T.; Tokumoto, M. *Chem. Lett.* **2000**, 406−407).
(5) Palacio, F.; Miller, J. S. *Nature* **2000**, *408*, 421−422.
(6) Kurmoo, M.; Graham, A. W.; Day, P.; Coles, S. J.; Hursthouse, M. B.; Caulfield, J. L.; Singleton, J.; Pratt, F. L.; Hayes, W.; Ducasse, L.; Guionneau, P. *J. Am. Chem. Soc.* **1995**, *117*, 12209−12217.
(7) Coronado, E.; Galán-Mascarós, J. R.; Gómez-García, C. J.; Laukhin, V. N. *Nature* **2000**, *408*, 447−449.
(8) (a) Kobayashi, A.; Udagawa, T.; Tomita, H.; Naito, T.; Kobayashi, H. *Chem. Lett.* **1993**, 2179−2182. (b) Kobayashi, H.; Tomita, H.; Naito, T.; Kobayashi, A.; Sakai, F.; Watanabe, T.; Cassoux, P. *J. Am. Chem. Soc.* **1996**, *118*, 368−377. (c) Brossard, L.; Clerac, R.; Coulon, C.; Tokumoto, M.; Ziman, T.; Petrov, D. K.; Laukhin, V. N.; Naughton, M. J.; Audouard, A.; Goze, F.; Kayashi, A.; Kobayashi, H.; Cassoux, P. *Eur. Phys. J.* **1998**, *B1*, 439−452.
(9) Kobayashi, H.; Kobayashi, A.; Cassoux, P. *Chem. Soc. Rev.* **2000**, *29*, 325−333.
(10) (a) Ojima, E.; Fujiwara, H.; Kato, K.; Kobayashi, H.; Kobayashi, A.; Tokumoto, M.; Cassoux, P. *J. Am. Chem. Soc.* **1999**, *121*, 5581−5582. (b) Fujiwara, H.; Fjiwara, E.; Nakazawa, Y.; Narymbetov, B. Z.; Kato, K.; Kobayashi, H.; Kobayashi, A.; Tokumoto, M.; Cassou, P. *J. Am. Chem. Soc.* **2001**, *123*, 306−314.
(11) Zhang, B.; Tanaka, H.; Fujiwara, H.; Kobayashi, H.; Fujiwara, E.; Kobayashi, A. *J. Am. Chem. Soc.* **2002**, *124*, 9982−9983.
(12) Fujiwara, H.; Kobayashi, H.; Fujiwara, E.; Kobayashi, A. *J. Am. Chem. Soc.* **2002**, *124*, 6816−6817.
(13) (a) Uji, S.; Shinagawa, H.; Terashima, T.; Terakura, C.; Yakabe, T.; Terai, Y.; Tokumoto, M.; Kobayashi, A.; Tanaka, H.; Kobayashi, H. *Nature* **2001**, *410*, 908−910. (b) Balicas, L.; Brooks, J. S.; Storr, K.; Uji, S.; Tokumoto, M.; Tanaka, H.; Kobayashi, H.; Kobayashi, A.; Barzykin, V.; Gor'kov, L. P. *Phys. Rev. Lett.* **2001**, *87*, 067002-1−067002-4.
(14) (a) Kobayashi, H.; Sato, A.; Arai, E.; Akutsu, H.; Kobayshi, A.; Cassoux, P. *J. Am. Chem. Soc.* **1997**, *119*, 12392−12393. (b) Sato, A.; Ojima, E.; Akutsu, H.; Kobayashi, A.; Cassoux, P. *Chem. Lett.* **1998**, 673−674.
(15) Imakubo, T.; Sawa, H.; Tajima, H.; Kato, R. *Synth. Met.* **1997**, *86*, 2047−2048.
(16) Tamura, M.; Matsuzaki, F.; Nishio, Y.; Kajita, K.; Kitazawa, T.; Mori, H.; Tanaka, S. *Synth. Met.* **1999**, *102*, 1716−1717.
(17) Tamura, M.; Yamanaka, K.; Mori, Y.; Nishio, Y.; Kajita, K.; Mori, H.; Tanaka, S.; Yamaura, J.-I.; Imakubo, T.; Kato, R.; Misaki, Y.; Tanaka, K. *Synth. Met.* **2001**, *120*, 1041−1042.
(18) Kushch, N. D.; Kazheva, O. N.; Grritsenko, V. V.; Buravov, L. I.; Van, K. V.; Dyachenko, O. A. *Synth. Met.* **2001**, *123*, 171−177.

Table 1. Crystallographic Data of $(BDT\text{-}TTP)_6[Ce(NO_3)_6](C_2H_5OH)_x$ ($x \approx 3$) and $(BDT\text{-}TTP)_5[Ln(NO_3)_5]$ (Ln = Tb, Dy, Ho, Er, Tm, Yb, Lu)

	Ln							
	Ce	Tb	Dy	Ho	Er	Tm	Yb	Lu
cryst syst	triclinic	triclinic	triclinic	triclinic	triclinic	triclinic	triclinic	triclinic
space group	$P\bar{1}$	$P\bar{1}$	$P\bar{1}$	$P\bar{1}$	$P\bar{1}$	$P\bar{1}$	$P\bar{1}$	$P\bar{1}$
a, Å	11.419(8)	11.561(4)	11.5795(5)	11.5529(4)	11.5522(4)	11.563(2)	11.5546(5)	11.553(3)
b, Å	12.289(7)	19.545(6)	19.5990(10)	19.5431(11)	19.5395(13)	19.552(4)	19.546(2)	19.539(6)
c, Å	20.82(2)	21.935(6)	21.9999(10)	21.922(3)	21.925(3)	21.927(4)	21.917(3)	21.913(6)
α, deg	74.97(3)	68.757(9)	68.706(4)	68.700(3)	68.690(3)	68.688(6)	68.680(4)	68.662(9)
β, deg	87.29(3)	76.727(10)	76.718(2)	76.713(2)	76.722(3)	76.720(8)	76.732(2)	76.750(2)
γ, deg	68.52(3)	78.848(11)	78.7536(13)	78.8862(13)	78.907(2)	78.956(8)	78.951(2)	78.960(12)
V, Å^3	2622	4463	4493	4455	4455	4463	4456	4453
Z	1	2	2	2	2	2	2	2
no. of rflns								
measd	21 631	37 389	26 524	26 257	26 509	37 061	26 546	37 403
obsd (used)	11 857	20 229	13 589	13 444	13 525	20 206	13 517	20 244
D_c, g cm^{-3}	1.878	1.765	1.762	1.773	1.774	1.773	1.778	1.781
R^a	0.089	0.082	0.073	0.077	0.074	0.068	0.078	0.074
$R_w{}^a$	0.076	0.105	0.103	0.106	0.103	0.093	0.105	0.092

[a] $R = \sum||F_o| - |F_c||/\sum|F_o|$; $R_w = [\sum w(|F_o| - |F_c|)^2/\sum wF_o^2]^{1/2}$.

reported the crystal structures.[19] These salts were metallic down to liquid He temperature. The Eu and Sm salts exhibited weakly temperature dependent, large paramagnetic susceptibilities, and $(BDT\text{-}TTP)_5[Ln(NO_3)_5]$ (Ln = Sm, Eu) were rare examples of organic metals, which showed large Van Vleck paramagnetism. The BDT-TTP donor with a tetrathiapentalene skeleton is known to yield a wide variety of highly conducting radical-cation salts.[20] In this paper, we present the details of the crystal structure, energy-band calculations, electrical conductivities, and magnetic susceptibilities of molecular conductors based on BDT-TTP with the heavy lanthanide nitrate complex $[Ln(NO_3)_x]$ (Ln = Tb, Dy, Ho, Er, Tm, Yb, Lu). The crystal structure and physical properties of a new lanthanide nitrate complex, $(BDT\text{-}TTP)_6[Ce(NO_3)_6](C_2H_5OH)_x$ ($x \approx 3$), are also reported.

Experimental Section

Synthesis. The solvents were reagent grade and were freshly distilled prior to use. BDT-TTP was prepared according to the literature method.[21] Lanthanide nitrate complexes $[Ln(NO_3)x]$ (x = 5, 6; Ln = Tb, Dy, Ho, Er, Tm, Yb, Lu) were prepared by the reaction of $Ln(NO_3)_3$, $AgNO_3$, and $^nBu_4NI$ according to a similar procedure for the preparation of $Ln(SCN)_x(NO_3)_y$.[18] Plate-shaped crystals of $(BDT\text{-}TTP)_5[Ln(NO_3)_5]$ were grown by electrochemical oxidation as follows. An H-shaped glass cell equipped with two electrodes, which were 1 mm diameter platinum wires, was filled with 10 mL of a 90% chlorobenzene−10% ethanol mixed solvent containing 1.5−2 mg of BDT-TTP and the corresponding tetra-*n*-butylammonium salt of $[Ln(NO_3)_5]^{2-}$ as the supporting electrolyte, under an argon atmosphere at room temperature. Applying a constant current of 0.1 μA for 5−10 days yielded black, plate-shaped crystals, which were harvested on the anode and air-dried after washing with large amounts of ethanol and hexane.

Crystal Structure Determination. The crystal structures of $(BDT\text{-}TTP)_5[Ln(NO_3)_5]$ (Ln = Tb, Dy, Ho, Er, Tm, Yb, Lu) and $(BDT\text{-}TTP)_6[Ce(NO_3)_6](C_2H_5OH)_x$ ($x \approx 3$) were analyzed on a RIGAKU MERCURY CCD X-ray system at room temperature. Monochromated Mo Kα radiation ($\lambda = 0.7107$ Å) was used for all X-ray experiments. Non-hydrogen atoms were anisotropically refined. Hydrogen atoms were allocated on the calculated optimal positions but not refined.

All the calculations were performed using the crystallographic software package CrystalStructure.[22] Table 1 summarizes the experimental details and results of crystal structure analyses of $(BDT\text{-}TTP)_5[Ln(NO_3)_5]$ (Ln = Tb, Dy, Ho, Er, Tm, Yb, Lu) and $(BDT\text{-}TTP)_6[Ce(NO_3)_6](C_2H_5OH)_x$ ($x \approx 3$).

Electrical Resistivity Measurements. The conventional four-probe method was applied for the electrical resistivity measurements of the single crystals of $(BDT\text{-}TTP)_5[Ln(NO_3)_5]$ (Ln = Tb, Dy, Ho, Er, Tm, Yb, Lu) and that of $(BDT\text{-}TTP)_6[Ce(NO_3)_6](C_2H_5OH)_x$ ($x \approx 3$). Four gold wires (15 μm diameter) were bound to the crystals, which were typically $0.30 \times 0.2 \times 0.02$ mm^3, with conducting gold paste as current and voltage terminals. The resistivities were measured in a temperature range of 2−300 K along the longest crystal axis and coincided with the crystallographic *b* axes of $(BDT\text{-}TTP)_5[Ln(NO_3)_5]$ and $(BDT\text{-}TTP)_6[Ce(NO_3)_6](C_2H_5OH)_x$ ($x \approx 3$).

Magnetic Susceptibility Measurements. The magnetic susceptibilities of $(BDT\text{-}TTP)_5[Ln(NO_3)_5]$ salts were measured on an MPMS-XL7 SQUID susceptometer (Quantum Design, Inc.) in the temperature range of 2−300 K and applied field of 0.5 T using randomly oriented polycrystalline samples. The magnetic properties of the Lu salt were not measured because of the diamagnetism of the Lu^{3+} ion. The paramagnetic susceptibilities, χ, were calculated by subtracting the diamagnetic contributions obtained assuming Pascal's law. The ac susceptibility of Er (127 Hz) and dc susceptibility of Ho salts were also measured at 0.05−1 K by using a homemade susceptometer and applied field of 0.51 T.

Results and Discussion

Crystal Structure. X-ray crystallographic data for an isostructural series of 11 salts of $(BDT\text{-}TTP)_5[Ln(NO_3)_5]$ (Ln = Nd, Sm, Eu, Gd, Tb, Dy, Ho, Er, Tm, Yb, Lu) were

(19) Otsuka, T.; Cui, H. B.; Kobayashi, A.; Misaki, Y.; Kobayashi, H. *J. Solid State Chem.* **2002**, *168*, 444−449.
(20) Misaki, Y.; Fujiwara, H.; Yamabe, T.; Mori, T.; Mori, H.; Tanaka, S. *Chem. Lett.* **1994**, 1653−1656.
(21) (a) Misaki, Y.; Nishikawa, H.; Kawakami, K.; Koyanagi, S.; Yamabe, T.; Shiro, M. *Chem. Lett.* **1992**, 2321−2324. (b) Misaki, Y.; Matsui, T.; Kawakami, K.; Nishikawa, H.; Yamabe, T.; Shiro, M. *Chem. Lett.* **1993**, 1337−1340.
(22) CrystalStructure 3.10: Crystal Structure Analysis Package; Rigaku and Rigaku/MSC, 2000−2002.

Table 2. Bond Lengths of O−N and Ln−O (Å)

	Ln										
	Nd	Sm	Eu	Gd	Tb	Dy	Ho	Er	Tm	Yb	Lu
O(1)−N(1)	1.19(3)	1.22(2)	1.20(3)	1.17(3)	1.21(2)	1.21(2)	1.21(3)	1.22(3)	1.23(1)	1.20(3)	1.22(3)
O(2)−N(1)	1.24(4)	1.22(2)	1.22(4)	1.22(3)	1.23(3)	1.24(2)	1.24(3)	1.23(3)	1.25(2)	1.21(3)	1.24(3)
O(3)−N(1)	1.25(4)	1.24(3)	1.25(4)	1.26(3)	1.22(2)	1.25(3)	1.25(3)	1.25(3)	1.23(2)	1.23(4)	1.24(3)
O(4)−N(2)	1.12(5)	1.20(2)	1.22(4)	1.22(4)	1.19(2)	1.20(2)	1.20(3)	1.20(3)	1.22(2)	1.18(4)	1.23(3)
O(5)−N(2)	1.22(4)	1.28(2)	1.24(4)	1.22(3)	1.26(2)	1.27(2)	1.26(3)	1.25(3)	1.27(2)	1.21(3)	1.24(3)
O(6)−N(2)	1.27(4)	1.26(3)	1.27(4)	1.27(4)	1.24(3)	1.26(3)	1.24(3)	1.25(3)	1.26(2)	1.25(4)	1.23(3)
O(7)−N(3)	1.17(5)	1.23(2)	1.18(4)	1.23(4)	1.23(2)	1.24(3)	1.24(3)	1.25(3)	1.24(2)	1.25(4)	1.27(3)
O(8)−N(3)	1.30(4)	1.25(2)	1.29(4)	1.28(3)	1.26(2)	1.26(2)	1.26(3)	1.28(3)	1.27(2)	1.25(4)	1.26(3)
O(9)−N(3)	1.26(4)	1.28(2)	1.24(4)	1.24(3)	1.25(2)	1.26(2)	1.27(3)	1.24(3)	1.27(2)	1.21(4)	1.19(3)
O(10)−N(4)	1.27(4)	1.28(3)	1.25(4)	1.21(4)	1.22(3)	1.22(3)	1.21(3)	1.22(3)	1.24(2)	1.21(3)	1.25(3)
O(11)−N(4)	1.17(5)	1.17(3)	1.20(4)	1.22(4)	1.17(3)	1.21(3)	1.21(3)	1.22(3)	1.20(2)	1.21(4)	1.22(3)
O(12)−N(4)	1.17(4)	1.25(3)	1.17(4)	1.19(4)	1.24(3)	1.22(3)	1.22(3)	1.22(3)	1.28(2)	1.22(3)	1.22(3)
O(13)−N(5)	1.20(4)	1.19(2)	1.25(3)	1.21(3)	1.22(2)	1.19(2)	1.22(3)	1.21(3)	1.21(1)	1.22(3)	1.19(3)
O(14)−N(5)	1.28(4)	1.19(2)	1.22(4)	1.24(3)	1.21(2)	1.22(2)	1.22(3)	1.22(3)	1.21(2)	1.22(4)	1.25(3)
O(15)−N(5)	1.29(4)	1.28(2)	1.26(3)	1.28(3)	1.27(2)	1.27(2)	1.27(3)	1.27(3)	1.26(2)	1.25(3)	1.27(3)
Ln−O(2)	2.53(3)	2.47(2)	2.41(3)	2.47(3)	2.43(2)	2.42(2)	2.40(2)	2.38(2)	2.368(11)	2.38(3)	2.33(2)
Ln−O(3)	2.55(3)	2.50(2)	2.49(2)	2.51(2)	2.46(2)	2.47(2)	2.47(2)	2.44(2)	2.411(11)	2.41(3)	2.40(2)
Ln−O(5)	2.54(3)	2.49(2)	2.43(3)	2.49(2)	2.43(2)	2.43(2)	2.42(2)	2.40(2)	2.382(11)	2.40(3)	2.35(2)
Ln−O(6)	2.53(3)	2.52(2)	2.47(3)	2.48(2)	2.46(2)	2.48(2)	2.42(2)	2.45(2)	2.435(11)	2.44(3)	2.39(2)
Ln−O(8)	2.56(2)	2.52(2)	2.48(2)	2.49(2)	2.44(2)	2.48(2)	2.44(2)	2.43(2)	2.426(10)	2.43(2)	2.40(2)
Ln−O(9)	2.56(3)	2.50(2)	2.43(3)	2.46(2)	2.44(2)	2.45(2)	2.41(2)	2.41(2)	2.405(10)	2.37(2)	2.35(2)
Ln−O(11)	2.47(3)	2.46(2)	2.44(3)	2.45(3)	2.40(2)	2.46(2)	2.42(2)	2.39(2)	2.392(12)	2.37(3)	2.32(2)
Ln−O(12)	2.53(3)	2.48(2)	2.46(3)	2.47(2)	2.43(2)	2.44(2)	2.44(2)	2.41(2)	2.375(11)	2.40(3)	2.34(2)
Ln−O(14)	2.56(3)	2.57(2)	2.51(3)	2.53(2)	2.49(2)	2.52(2)	2.49(2)	2.48(2)	2.470(11)	2.44(2)	2.44(2)
Ln−O(15)	2.52(2)	2.51(2)	2.44(3)	2.47(2)	2.43(2)	2.45(2)	2.42(2)	2.41(2)	2.396(11)	2.36(2)	2.36(2)

obtained by combining the results of this work with previously reported structural data.[19] The crystals of $(BDT\text{-}TTP)_5[Ln(NO_3)_5]$ with a 5:1 donor composition belonged to a triclinic crystal system with a $P\bar{1}$ space group and were isostructural. Table 1 lists the cell parameters at room temperature (293 K). Figure 1 shows the crystal structures of $(BDT\text{-}TTP)_5[Ln(NO_3)_5]$. In each unit cell there are five kinds of crystallographically independent donor molecules and one $[Ln(NO_3)_5]^{2-}$ anion. For $(BDT\text{-}TTP)_5[Tm(NO_3)_5]$, the dihedral angle between the molecular planes of the five donor molecules (A−E) were between 0.15 and 0.70° and the five BDT-TTP molecules were stacked face to face to form a column along the $[1\bar{1}0]$ direction, in which two pentads are connected with each other by an inversion center (see Figure 1), forming a 10-fold columnar structure.

There were many short S···S contacts between the BDT-TTP molecular columns. For example, in the Tm^{3+} salt the distances were 3.569, 3.617, 3.629, 3.636, and 3.683 Å. These lateral and intercolumnar S···S contacts resulted in a two-dimensional sheetlike structure of BDT-TTP molecules.

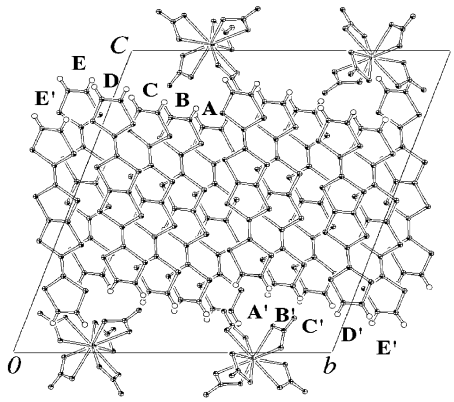

Figure 1. Crystal structure of $(BDT\text{-}TTP)_5[Tm(NO_3)_5]$.

The $[Ln(NO_3)_5]^{2-}$ anions are separately allocated between the BDT-TTP sheets. Figure 2 shows the structure of the $[Ln(NO_3)_5]^{2-}$ anion. Heavy lanthanide ions are surrounded by five bidentate NO_3^- ligands so that the Ln^{3+} ions had a 10-O-coordinated structure, which is essentially the same as the coordination structure of $(BDT\text{-}TTP)_5[Ln(NO_3)_5]$ (Ln = Sm, Eu, Nd, Gd).[19] The structural data for the Tm salt can explain the structure of $[Ln(NO_3)_5]^{2-}$. The three NO_3^- ligands were almost in the same plane (see Figure 2), and five NO_3^- planes surrounded the Tm^{3+} ion (F−J). The dihedral angle between the planes F and H (which was formed by NO_3^- and the central metal ion) was 23.21°, and that between planes F and G was 15.72°. The remaining two NO_3^- ligands, I and J, were nearly perpendicular to these planes (the dihedral angles were 69.71−98.26°). These two planes were orthogonal (the dihedral angle is 91.43°). The O−N distance is 1.20(2)−1.28(2) Å, and the Ln−O distance is 2.368(11)−2.470(11) Å (see Table 2), and ∠O−N−O = 113.4(11)−124.6(16)° and ∠O−Ln−O = 50.7(4)−52.9(3)° (see Table

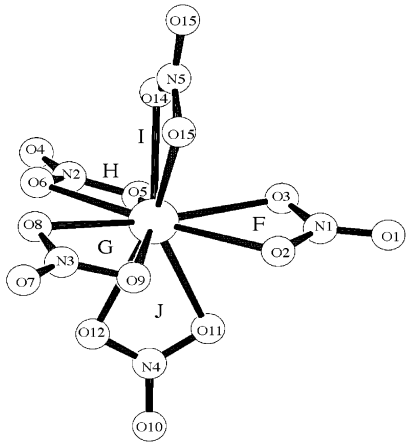

Figure 2. Anion structure of $[Tm(NO_3)_5]^{2-}$.

Table 3. Bond Angles of ∠O−N−O and ∠O−Ln−O (deg)

	Ln										
	Nd	Sm	Eu	Gd	Tb	Dy	Ho	Er	Tm	Yb	Lu
O(1)−N(1)−O(2)	119.8(43)	122.4(26)	124.9(40)	122.0(37)	121.2(25)	123.2(25)	121.9(30)	123.3(29)	122.5(15)	121.9(38)	121.8(33)
O(1)−N(1)−O(3)	121.5(40)	122.3(24)	121.3(34)	123.2(32)	123.8(24)	123.8(23)	123.9(26)	123.4(26)	124.1(14)	126.0(35)	126.5(30)
O(2)−N(1)−O(3)	118.7(32)	115.3(20)	113.7(27)	114.9(28)	114.9(18)	113.1(19)	114.2(22)	113.3(21)	113.4(11)	112.1(30)	111.7(24)
O(4)−N(2)−O(5)	130.9(48)	120.5(25)	124.1(45)	123.1(37)	122.9(25)	122.5(25)	123.0(31)	123.8(30)	121.8(16)	124.0(40)	121.2(35)
O(4)−N(2)−O(6)	124.4(44)	124.8(22)	122.2(41)	125.5(30)	124.3(22)	124.4(22)	125.0(28)	123.6(27)	123.1(14)	126.2(33)	123.7(30)
O(5)−N(2)−O(6)	104.6(43)	114.6(21)	113.3(33)	111.3(32)	112.7(19)	113.1(21)	112.0(25)	112.5(25)	115.1(12)	109.7(36)	115.1(27)
O(7)−N(3)−O(8)	126.8(41)	123.0(22)	124.8(35)	124.5(31)	124.3(21)	122.9(22)	124.3(27)	122.4(26)	121.1(14)	122.0(34)	119.2(30)
O(7)−N(3)−O(9)	127.3(40)	121.9(22)	127.1(36)	125.3(33)	122.6(22)	123.8(22)	123.7(26)	125.8(25)	123.6(14)	126.4(34)	124.3(29)
O(8)−N(3)−O(9)	105.8(44)	115.1(20)	107.8(31)	110.1(32)	113.1(18)	113.3(21)	111.9(25)	111.8(25)	115.2(12)	111.5(38)	116.1(30)
O(10)−N(4)−O(11)	125.0(44)	127.8(28)	119.2(37)	123.3(37)	124.9(26)	122.1(25)	121.8(30)	122.5(29)	121.6(16)	123.8(36)	121.7(30)
O(10)−N(4)−O(12)	116.3(51)	115.2(29)	123.0(39)	122.8(40)	121.1(27)	123.7(27)	123.5(32)	123.3(30)	124.6(16)	124.5(37)	126.3(32)
O(11)−N(4)−O(12)	116.8(37)	115.5(22)	117.5(32)	113.8(29)	113.7(20)	113.9(21)	114.5(25)	113.9(22)	113.5(13)	111.7(28)	112.0(24)
O(13)−N(5)−O(14)	124.6(37)	123.1(22)	123.3(32)	124.2(30)	124.8(21)	123.7(21)	123.2(27)	123.5(25)	123.8(13)	123.2(32)	125.3(28)
O(13)−N(5)−O(15)	123.0(38)	119.6(22)	120.7(35)	121.7(33)	120.0(22)	122.0(22)	121.4(27)	122.1(26)	121.6(14)	125.3(34)	124.8(32)
O(14)−N(5)−O(15)	112.4(34)	117.3(19)	115.9(31)	114.1(29)	114.9(18)	114.2(19)	115.3(24)	114.3(24)	114.4(12)	111.3(30)	109.7(27)
O(2)−Ln−O(3)	49.8(9)	49.5(6)	49.8(9)	49.6(9)	49.9(6)	50.4(6)	51.0(7)	51.0(7)	51.3(4)	49.9(9)	51.3(8)
O(5)−Ln−O(6)	45.7(10)	50.6(6)	50.7(10)	48.8(9)	50.5(6)	51.1(6)	50.6(8)	50.8(8)	52.6(4)	49.3(10)	52.2(8)
O(8)−Ln−O(9)	47.0(9)	50.4(5)	49.0(8)	49.2(7)	50.9(5)	50.8(5)	51.0(6)	51.2(6)	52.9(3)	50.2(8)	52.0(7)
O(11)−Ln−O(12)	46.9(12)	49.0(8)	49.0(10)	48.6(10)	49.4(7)	49.2(7)	49.7(8)	50.3(8)	51.4(4)	49.9(10)	51.2(8)
O(14)−Ln−O(15)	49.6(9)	49.0(6)	50.4(9)	50.0(8)	50.3(6)	49.6(6)	50.6(7)	50.6(7)	50.7(4)	50.3(9)	50.8(8)

Table 4. Short Distances of S···O (Å)

	Ln										
	Nd	Sm	Eu	Gd	Tb	Dy	Ho	Er	Tm	Yb	Lu
S(1)···O(7)	3.40(4)	3.42(2)	3.48(3)	3.48(3)	3.45(2)	3.45(2)	3.46(3)	3.46(2)	3.46 (1)	3.49(3)	3.49(3)
S(2)···O(4)	3.27(3)	3.29(2)	3.32(3)	3.30(2)	3.31(2)	3.31(2)	3.31(2)	3.33(2)	3.336(12)	3.31(3)	3.36((2)
S(9)···O(4)	3.18(3)	3.20(2)	3.22(3)	3.23(2)	3.21(2)	3.23(2)	3.21(2)	3.24(2)	3.249(12)	3.24(3)	3.27(2)
S(17)···O(6)	3.54(3)	3.42(2)	3.46(3)	3.49(3)	3.45(2)	3.44(2)	3.48(2)	3.46(2)	3.438(12)	3.47(3)	3.47(3)
S(18)···O(10)	3.34(4)	3.34(2)	3.40(4)	3.40(3)	3.40(2)	3.39(2)	3.42(3)	3.43(3)	3.414(13)	3.41(3)	3.43(3)
S(39)···O(13)	3.38(3)	3.46(1)	3.43(2)	3.47(2)	3.48(2)	3.49(1)	3.48(2)	3.49(2)	3.518(9)	3.50(2)	3.50(2)
S(40)···O(1)	3.06(3)	3.09(2)	3.11(3)	3.12(2)	3.12(2)	3.10(2)	3.09(2)	3.11(2)	3.126(10)	3.11(2)	3.12(2)

Table 5. Shortest Distances of Ln···Ln and O···O (Å)

	Ln···Ln	O···O		Ln···Ln	O···O
La^{3+}			Tb^{3+}	9.986	6.47
Ce^{3+}	11.419	6.11	Dy^{3+}	10.014	6.46
Pr^{3+}			Ho^{3+}	9.988	6.38
Nd^{3+}	9.987	6.60	Er^{3+}	9.989	6.38
Sm^{3+}	9.998	6.53	Tm^{3+}	10.001	6.40
Eu^{3+}	9.834	6.41	Yb^{3+}	9.995	6.39
Gd^{3+}	10.054	6.42	Lu^{3+}	9.996	6.40

3). Rather short S···O contacts between BDT-TTP molecules and $Ln(NO_3)_5^{2-}$ anions existed: S(1)···O(7) = 3.45 Å, S(2)···O(4) = 3.31 Å, S(9)···O(4) = 3.23(2) Å, S(17)···O(6) = 3.44 Å, S(18)···O(10) = 3.39 Å, S(39)···O(13) = 3.49 Å, and S(40)···O(1) = 3.10 Å. Table 4 lists the S···O distances for the other salts. The Ho crystal displayed the shortest Ln···Ln distance, 9.988 Å, and the shortest O···O distance between the neighboring anions, 6.09 Å (Table 5).

The crystal of $(BDT\text{-}TTP)_6[Ce(NO_3)_6](C_2H_5OH)_x$ ($x \approx 3$) belongs to a triclinic crystal system with a $P\bar{1}$ space group. The x value was estimated by the population analysis of the crystal structure determination. Table 1 lists the cell parameters at room temperature (293 K). Figure 3 shows the crystal structures of the $(BDT\text{-}TTP)_6[Ce(NO_3)_6](C_2H_5OH)_x$ ($x \approx 3$) salt. Three donor molecules (A−C) and half of the $[Ce(NO_3)_6]^{3-}$ anion are crystallographically independent. The molecules A−C were nearly parallel, and the dihedral angles between the molecular planes were approximately 0.71°. Three BDT-TTP molecules are stacked face to face to form a 6-fold column along the [200] direction. The intermolecular distances were 3.465, 3.440, and 3.475 Å between plane A and plane A′, plane A and plane B, and plane B and plane C, respectively. Plane A′ is related to plane A by inversion symmetry. The C_2H_5OH molecules located between $[Ce(NO_3)_6]^{3-}$ anions were disordered. There were many short S···S contacts between BDT-TTP columns: S(5)···S(21) = 3.57(2) Å, S(7)···S(19) = 3.59(2) Å, S(13)···S(13) = 3.56(3) Å, and S(14)···S(14) = 3.53(3) Å.

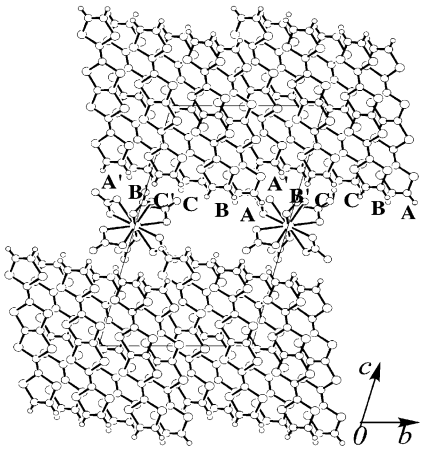

Figure 3. Crystal structure of $(BDT\text{-}TTP)_6[Ce(NO_3)_6](C_2H_5OH)_x$ ($x \approx 3$).

The $[Ce(NO_3)_6]^{3-}$ anions were separated by BDT-TTP sheets. Figure 4 shows the molecular structure of the $[Ce(NO_3)_6]^{3-}$ anion. The Ce^{3+} ions were surrounded by six bidentate NO_3^- ligands so that the Ce^{3+} ions had 12-O-coordinated structures. Three NO_3^- ligands were nearly perpendicular. The dihedral angles were 92.37, 91.67, and

Table 6. Overlap Integrals of $(BDT\text{-}TTP)_5Ln(NO_3)_5$ ($\times 10^3$)

	Ln										
	Nd	Sm	Eu	Gd	Tb	Dy	Ho	Er	Tm	Yb	Lu
a	21.27	22.51	22.56	21.24	22.19	22.01	22.65	21.96	22.33	21.73	22.10
b	−23.97	−23.77	−23.91	−22.34	−23.68	−23.55	−23.77	−23.67	−23.63	−23.52	−23.64
c	−23.82	−23.82	−24.42	−22.68	−23.63	−23.32	−23.73	−23.77	−23.42	−23.62	−23.75
d	−25.24	−24.83	−24.30	−23.76	−24.65	−24.07	−24.89	−24.61	−24.40	−24.62	−24.37
e	−24.79	−25.20	−25.18	−23.61	−25.57	−24.97	−24.48	−25.03	−24.74	−24.34	−25.24
f	24.42	24.24	24.67	23.31	24.96	24.55	23.87	24.18	24.18	22.73	24.68
g	2.16	2.19	2.02	2.17	2.01	2.21	2.30	2.19	2.30	2.39	2.34
h	7.68	7.80	7.99	7.98	7.82	7.54	8.12	7.89	7.93	7.68	7.60
i	1.52	1.38	1.44	1.58	1.48	1.60	1.60	1.55	1.59	1.78	1.62
j	−7.74	−7.86	−7.67	−7.57	−7.69	−7.45	−7.82	−7.77	−7.83	−7.79	−7.79
k	−0.20	−0.64	−0.49	−0.64	−0.63	−0.72	−0.64	−0.59	−0.80	−0.61	−0.75
l	−8.77	−8.67	−8.88	−8.65	−8.79	−8.51	−8.71	−8.93	−8.70	−8.73	−8.81
m	−0.41	−0.29	−0.22	−0.46	−0.37	−0.41	−0.25	−0.28	−0.36	−0.35	−0.47
n	−10.11	−9.75	−10.03	−9.76	−10.00	−9.66	−10.24	−10.05	−10.07	−10.09	−10.16
o	0.40	0.40	0.49	0.60	0.78	0.77	0.66	0.79	0.94	0.93	0.76
p	7.41	7.33	6.63	7.03	7.16	6.77	6.78	6.70	7.06	6.30	6.88
q	0.13	−0.15	−0.07	0.15	−0.20	0.14	−0.03	0.07	0.02	0.13	−0.04

86.88° between planes D and E, planes D and F, and planes E and F, respectively. N−O = 1.21(4)−1.33(5) Å, Ce−O = 2.43(5)−2.65(5) Å, ∠O−N−O = 111.5(57)−126.8(58)°, and ∠O−Ce−O = 47.5(11)−51.0(15)°. The large Ce−O distance relative to the Tm−O distances (2.37−2.47 Å) was consistent with a lanthanide contraction. The short S···O contacts between anions and BDT-TTP molecules were as follows: S(2)···O(4) = 3.43(3) Å, S(17)···O(4) = 3.45(3) Å, S(10)···O(7) = 3.06(4) Å.

Although the Pr salts could not be sufficiently examined, preliminary X-ray examination suggested the existence of two modifications.

Electronic Band Structure Calculations. The overlap integrals, electronic band structures, and Fermi surfaces for the series of $(BDT\text{-}TTP)_5[Ln(NO_3)_5]$ (Ln = Tb, Dy, Ho, Er, Tm, Yb, Lu) salts were calculated using the extended Hückel type tight-binding band approximation based on the room-temperature crystal structures. The following exponent *z* and the ionization potential (eV) were adopted: S 3s, 2.122, −19.99; S 3p, 1.827, −10.99; S 3d, 1.500, −5.44; C 2s, 1.625, −21.39; C2p, 1.625, −11.40; H 1s 1.0, −13.6. Figure 5 shows the donor arrangement of $(BDT\text{-}TTP)_5[Tm(NO_3)_5]$, and Table 6 lists the overlap integrals of $(BDT\text{-}TTP)_5[Tm(NO_3)_5]$, which were almost independent of the lanthanide ions (Tb, Dy, Ho, Er, Tm, Yb, Lu) and are approximately equal to those of light rare earth salts (Nd, Sm, Eu, Gd).[19] The overlap integrals along BDT-TTP columns were (22.33−24.74) × 10^{-3}, and the strongest intercolumnar transverse interactions were about 40% of the intracolumnar interactions. Consequently, $(BDT\text{-}TTP)_5[Ln(NO_3)_5]$ (Ln = Tb, Dy, Ho, Er, Tm, Yb, Lu) had two-dimensional energy dispersion curves. Since there were 10 dispersion curves, Figure 6 shows fairly complex Fermi surfaces of $(BDT\text{-}TTP)_5[Tm(NO_3)_5]$.

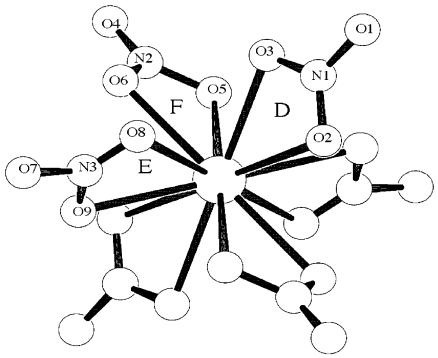

Figure 4. Anion structure of $[Ce(NO_3)_6]^{3-}$.

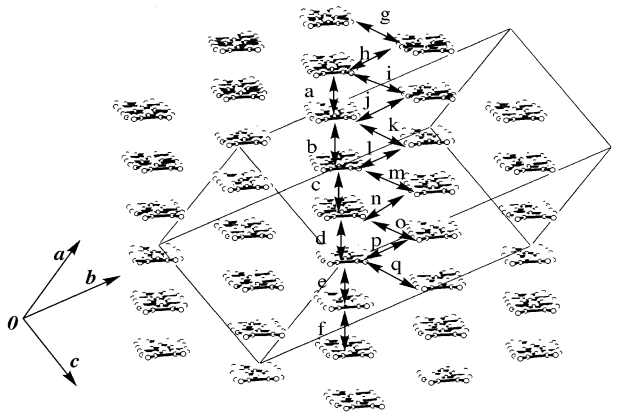

Figure 5. Donor arrangement of $(BDT\text{-}TTP)_5[Tm(NO_3)_5]$ viewed along the long axis of BDT-TTP.

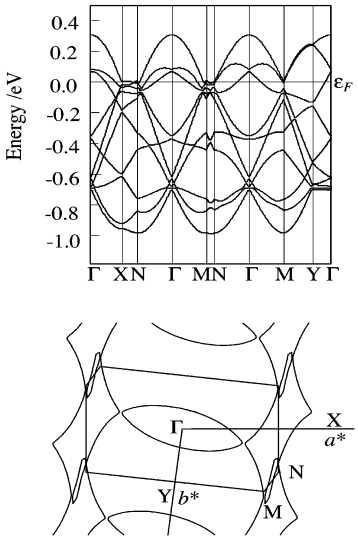

Figure 6. Band structure and Fermi surface of $(BDT\text{-}TTP)_5[Tm(NO_3)_5]$ calculated using the tight-binding approximation.

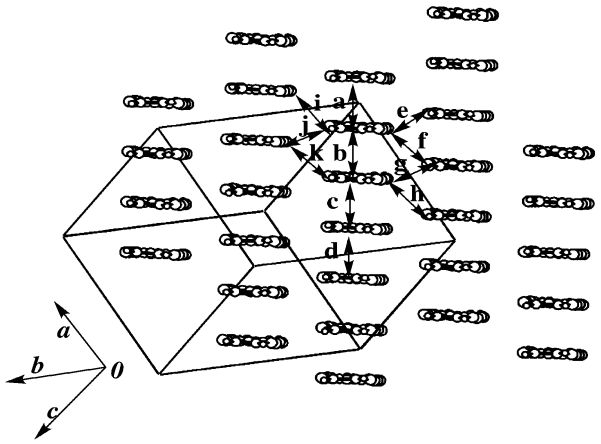

Figure 7. Donor arrangement of $(BDT\text{-}TTP)_6[Ce(NO_3)_6](C_2H_5OH)_x$ ($x \approx 3$) viewed along the long axis of BDT-TTP.

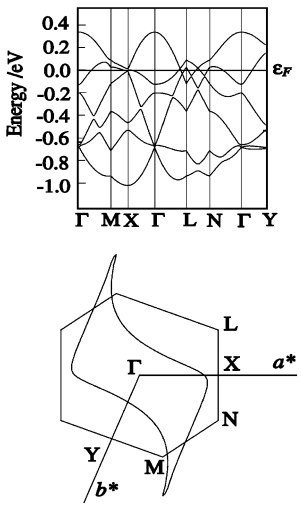

Figure 8. Band structure and Fermi surface of $(BDT\text{-}TTP)_6[Ce(NO_3)_6](C_2H_5OH)_x$ ($x \approx 3$) calculated using the tight-binding approximation.

Figure 7 shows the donor arrangement of $(BDT\text{-}TTP)_6[Ce(NO_3)_6](C_2H_5OH)_x$ ($x \approx 3$), and the electronic band structure of it is also shown in Figure 8. The general features of the band structure were very similar to those of $(BDT\text{-}TTP)_5[Ln(NO_3)_5]$, but the obtained Fermi surfaces were simpler because of the relatively small number of energy dispersion curves.

Electric Properties. Figure 9 summarizes the temperature dependencies of the resistivities of $(BDT\text{-}TTP)_x[Ln(NO_3)_y]$ ($x = y = 5, 6$; Ln = La, Ce, Tb, Dy, Ho, Er, Tm, Yb, Lu). The room-temperature resistivities were 2×10^{-3} Ω cm (Sm)[19] to 10^{-1} Ω cm (La, Er, and Lu). The resistivities of La, Er, Dy, and Lu salts, which had relatively large room-temperature resistivities (10^{-1} Ω cm (La, Er, and Lu), 5×10^{-2} Ω cm (Dy)), decreased as the temperature was lowered. The very broad and shallow La salt resistivity minimum around 20 K was not an intrinsic one. The Ho salt had a very small resistivity minimum, which was almost unnoticeable, around 2 K. The other samples showed a gradual decrease in resistivity as the temperature was lowered, which was consistent with the stable two-dimensional metallic properties suggested by the band structure calculations. The resistivities of Er, Tm, and Ho salts were measured down to

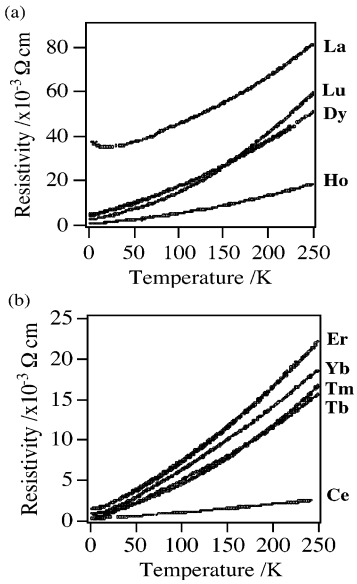

Figure 9. Temperature dependence of the resistivities of $(BDT\text{-}TTP)_x[Ln(NO_3)_y]$ ($x = y = 5, 6$): (a) Ln = La, Ho, Dy, Lu; (b) Ln = Er, Tb, Tm, Yb, Ce.

50 mK. Unlike the Er and Tm salts, which displayed constant residual resistivity, the Ho salt resistivity increased slightly as the temperature decreased and remained constant (or reached a maximum) around 200 mK. However, a clear anomaly, suggesting an electric transition, was not detected.

As shown in Figure 9b, $(BDT\text{-}TTP)_6[Ce(NO_3)_6](C_2H_5OH)_x$ ($x \approx 3$) was also metallic down to 2 K (ρ(RT) = 5×10^{-3} Ω cm).

Magnetic Properties. The magnetic properties of $(BDT\text{-}TTP)_5[Ln(NO_3)_5]$ with light lanthanide ions (Ln = Nd, Sm, Eu, Gd) were recently reported.[19] The Eu and Sm salts exhibited large Van Vleck paramagnetism (2×10^{-3} emu mol^{-1} (Sm), 5×10^{-3} emu mol^{-1} (Eu)). Figure 10a plots the temperature dependencies of the susceptibilities of $(BDT\text{-}TTP)_5[Ln(NO_3)_5]$ with heavy rare-earth ions (Ln = Tb, Dy, Ho, Er, Tm, Yb), and Figure 10b shows their χT *vs* *T* plots.

The susceptibility of Tb^{3+} ($S = L = 3$, $J = 6$) salt showed a Curie−Weiss behavior with $C = 9.86$ emu K mol^{-1} and $\Theta = -2.1$ K. The C value gave $g_{eff} = 1.37$ ($C = N\mu_B{}^2 g_{eff}{}^2 S(S+1)/3k_B$), which approximately equaled the calculated g value (g_J) of 1.5 ($g_J = {}^3/_2 + [S(S+1) - L(L+1)]/2J(J+1)$). The paramagnetic contribution of the π conduction electrons, which is approximately 5×10^{-4} emu mol^{-1} in a typical organic metal system, was much smaller than the susceptibility due to the localized moments of Ln^{3+}. Similar Curie−Weiss analyses of the susceptibilities were made on Dy^{3+} ($S = {}^5/_2$, $L = 5$, $J = {}^{15}/_2$), Ho^{3+} ($S = {}^5/_2$, $L = 5$, $J = 8$), Er^{3+} ($S = {}^3/_2$, $L = 6$, $J = {}^{15}/_2$), Tm^{3+} ($S = 1$, $L = 5$, $J = 6$), and Yb^{3+} ($S = {}^1/_2$, $L = 3$, $J = {}^7/_2$) salts: Dy^{3+}, $C = 8.65$ emu K mol^{-1}, $\Theta = -1.3$ K, $g_{eff} = 1.04$, $g_J = 1.33$; Ho^{3+}, $C = 12.35$ emu K mol^{-1}, $\Theta = -15.1$ K, $g_{eff} = 1.17$, $g_J = 1.25$; Er^{3+}, $C = 8.47$ emu K mol^{-1}, $\Theta = -3.8$ K, $g_{eff} = 1.06$, $g_J = 1.2$; Tm^{3+}, $C = 4.79$ emu K mol^{-1}, $\Theta = -8.4$ K, $g_{eff} = 0.96$, $g_J = 1.17$; Yb^{3+}, $C = 1.34$ emu K mol^{-1}, $\Theta = -0.2$ K, $g_{eff} = 0.82$, $g_J = 1.14$.

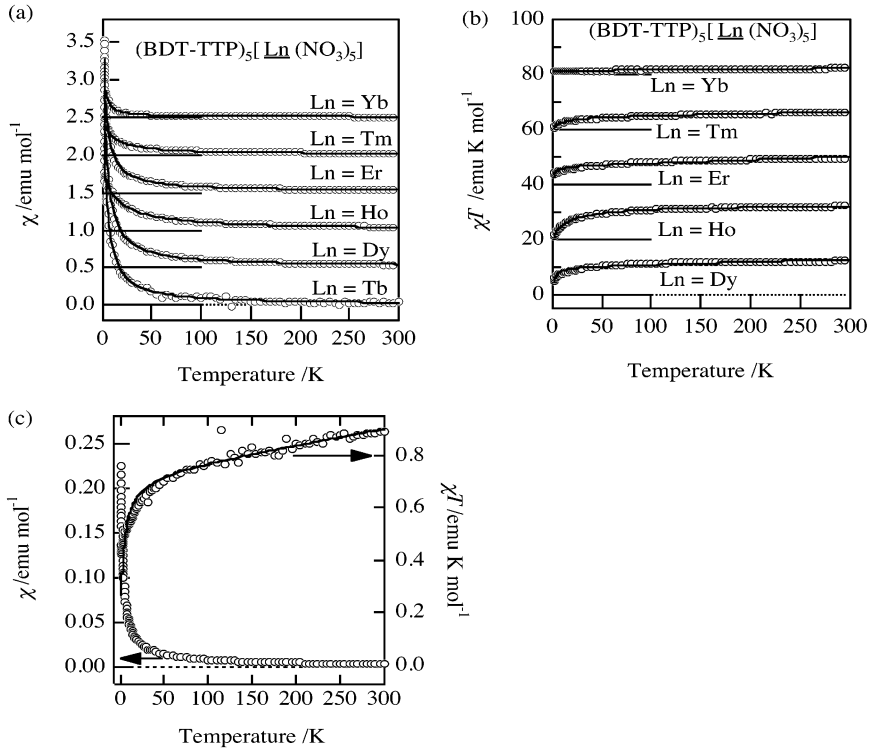

Figure 10. Temperature dependence of (a) the magnetic susceptibilities of $(BDT\text{-}TTP)_5[Ln(NO_3)_5]$ (Ln = Tb, Dy, Ho, Er, Tm, Yb, Lu) and (b) their χT vs T plots (the plot of the Tb salt was omitted, owing to its noisy signals) and (c) the magnetic susceptibility of $(BDT\text{-}TTP)_6[Ce(NO_3)_6](C_2H_5OH)_x$ ($x \approx 3$) and its χT vs T plot.

As shown in Figure 10a, the susceptibility of the Ho^{3+} salt was well reproduced by the Curie−Weiss law at 2−300 K and resulted in a comparatively large $|\Theta|$ of 15 K. Although the comparatively large antiferromagnetic interaction suggested from the $|\Theta|$ value and the χT *vs* T plot (Figure 10b) seemed to contradict the traditional image of strongly localized 4f orbitals shielded by the electrons in the outer 5s and 5p orbitals, an ideal Curie−Weiss fitting for such a wide temperature range appears not to be accidental. The isostructural properties and similar magnitudes of the magnetic moment of the Dy^{3+} salt with a small $|\Theta|$ value indicates that the dipole interactions between the magnetic moments of Ln^{3+} ions do not play an important role in producing the comparatively large $|\Theta|$ value of the Ho^{3+} salt. On the other hand, since the shortest contact between anions (O···O) was greater than 6.0 Å, this indicates that direct antiferromagnetic interactions between neighboring lanthanide anions through the overlapping of ligand orbitals was negligible. Thus, it is possible that the 4f orbitals of the Ho atoms are sensitive to the ligand field. This sensitivity would result in an Ho^{3+} ion orbital moment and/or would produce a small amount of mixing between 4f and ligand orbitals to give rise to "real" intermolecular antiferromagnetic interactions through the intermolecular overlapping between π (BDT-TTP) and ligand orbitals. The low-temperature susceptibilities on Ho and Er salts were measured at 0.05−1.0 K. Although a slight anomaly of the curvature of the temperature dependence of the susceptibilities was detected on the Ho crystals around 100 mK, clear evidence for a magnetic transition was not detected. The susceptibilities of Ho and Er gradually increased as the temperature was decreased to 50 mK.

The susceptibilities of $(BDT\text{-}TTP)_6[Ce(NO_3)_6](C_2H_5OH)_x$ ($x \approx 3$) were also measured at 2−300 K. As shown in Figure 10c, the susceptibilities are well reproduced by the Curie−Weiss plot: $C = 0.72$ emu mol^{-1} and $\Theta = -1.4$ K. The g_{eff} value of 0.78 is approximately equal to a g_J value of 0.86 ($S = {}^1/_2$, $L = 3$, $J = {}^5/_2$). Thus, the general feature of susceptibility of BDT-TTP conductors with lanthanide nitrate anions can be explained by the magnetic nature of the lanthanide ions.

Conclusion

Organic metals with lanthanide nitrato complex anions $[Ln(NO_3)_5]^{2-}$ (Ln = Tb, Dy, Ho, Er, Yb, Lu) were prepared using the π-donor molecules BDT-TTP. The crystal structures of organic metals for a complete series of lanthanide nitrato anions, except for Pr and Pm complex anions, were obtained by combining recently reported $(BDT\text{-}TTP)_5[Ln(NO_3)_5]$ (Ln = Nd, Sm, Eu, Gd) data and newly obtained $(BDT\text{-}TTP)_6[Ce(NO_3)_6](C_2H_5OH)_x$ ($x \approx 3$) data. Five different crystallographically independent donor molecules and one kind of $[Ln(NO_3)_5]^{2-}$ anion were observed in an asymmetric unit of $(BDT\text{-}TTP)_5[Ln(NO_3)_5]$. The BDT-TTP molecules were stacked face to face in a column along the $[1\bar{1}0]$ direction. The $[Ln(NO_3)_5]^{2-}$ anions were sandwiched between the BDT-TTP sheets, and there were no short contacts between neighboring anions. Except for the crystal of $(BDT\text{-}TTP)_5[La(NO_3)_5]$, which exhibited a small resistivity minimum probably due to lattice defects, all the examined

crystals were metallic down to 2 K, which was consistent with the two-dimensional nature of the electronic band structures of $(BDT\text{-}TTP)_5[Ln(NO_3)_5]$ and $(BDT\text{-}TTP)_6[Ce(NO_3)_6](C_2H_5OH)_x$ ($x \approx 3$). All the salts displayed large paramagnetism that originated from the Ln^{3+} ions. The temperature dependence of the magnetic susceptibilities of $(BDT\text{-}TTP)_5[Ho(NO_3)_5]$ was well reproduced by a Curie−Weiss plot at 2−300 K and resulted in a comparatively large Weiss temperature ($|\Theta|$) of 15 K.

Acknowledgment. This work was supported by a Grant-in-Aid for Scientific Research (S) (Grant No. 14103005) and for the 21st Century COE Program for Frontiers in Fundamental Chemistry from the Ministry of Education, Culture, Sports, Science and Technology of Japan. This work was also supported by CREST (Core Research for Evolutional Science and Technology of JST (Japan Science and Technology Coporation)).

Supporting Information Available: Twelve X-ray crystallographic files, in CIF format. This material is available free of charge via the Internet at http://pubs.acs.org.

IC034459G